

Classical Myelo-Proliferative Neoplasms emergence and development based on real life incidence and mathematical modeling

Ana Fernández Baranda¹, Vincent Bansaye¹, Evelyne Lauret², Morgane Mounier³,
Valérie Ugo⁴, Sylvie Méléard^{*, 1, 5}, and Stéphane Giraudier^{*, 6}

* These two authors are co-last authors.

¹CMAP, CNRS, Ecole Polytechnique, Institut Polytechnique de Paris, 91128, Palaiseau, France

²Université de Paris, Institut Cochin, INSERM U1016, CNRS UMR8104, F-75014 PARIS, France

³Malignant Hemopathies Registry of cote d'Or, INSERM U1231, CHU Dijon Bourgogne, Dijon, France

⁴Univ Angers, Nantes Université, CHU Angers, INSERM, CNRS, CRCI2NA, F-49000 Angers, France

⁵Institut universitaire de France

⁶Université Paris-Cité, Hôpital Saint Louis, INSERM U1131, F-75010 Paris, France

Short title: Modeling MPN development (24 characters)

Corresponding author: Stéphane Giraudier

Address: INSERM U1131, Centre Hayem, Hôpital Saint Louis, 1 avenue Claude Vellefaux, 75010 Paris, France. e-mail: stephane.giraudier@aphp.fr

Supported by grants from the INSERM and INCa 2018.

Significant Statement

We demonstrate using progressively complexified models that the rate of active mutation occurrence is not constant and doesn't just rely on individual variability, but rather should be linked to an aging mechanism. *A contrario*, the expansion time can be considered as constant. Lastly, comparing the two main JAK2V617F pathologies, we noticed that the first period of time (rate of active homozygous mutation occurrence) for Polycythemia Vera takes approximately 1.5 years more than for Essential Thrombocytemia to develop when the expansion time was quasi-similar.

INTRODUCTION

When does cancer begin? This is a biological question but also one of the most frequent questions of patients when a cancer diagnosis is confirmed. This is also a recurrent question in medicine based on the hypothesis that the sooner the cancer diagnosis is performed, the easier the treatment. Myeloproliferative disorders are chronic disorders issued from the transformation of hematopoietic stem cell and related to the acquisition of JAK2 signaling deregulation, (JAK2V617F mutation being the most frequent, or mutations of JAK2 exon12, CALR or MPL). Three pathologies emerged as main MPN: Essential Thrombocythemia (ET) characterized by an increased platelet number and a JAK2 mutation in one allele (when JAK2 mutation is responsible for the ET development), Polycythemia Vera (PV) (erythroid compartment enlargement) that is characterized by the acquisition of the JAK2 mutation in more than 90% of cases, followed by an homologous recombination of JAK2V617F and last, myelofibrosis that can be secondary to the two first MPN or primary and is often characterized by JAK2 mutation and association of secondary events (TET₂ mutation, ASXL1 mutation etc. . .)¹. When a diagnosis of MPN just like Polycythemia Vera is performed, the total tumor mass (erythrocytes) represents at least 25% of the erythroid hematopoietic mass (definition of the needed increased Red Cell Mass to diagnose a polycythemia)². This suggests a total cancer mass of at least 750 grams in the blood and probably the same mass in the bone marrow. Based on the cell mass, we can speculate that a minimum of one million cell divisions are needed to create such a MPN. We also can speculate that the same order or tumor mass is present in all myeloid chronic myeloproliferative malignancies as previously described in Chronic Myeloid Leukemia (CML) (Diagnosis is performed when the tumor mass reach 10¹² cells and with a median 2,3ng /cell, the tumor mass can be estimated in the same order of magnitude as PV; and ET probably). This tumor mass growth takes time. Based on the speed of divisions and the time for mutation emergence, it is possible to estimate the time of emergence based on the time of diagnosis. Different approaches have been proposed in the literature to calculate this delay. They all are based on mathematical modeling of two compounds: Time for a first cell harboring the JAK2V617F mutation to emerge and enter the cell cycle (T_1 , time of active mutation emergence) and time for cancer population to grow until diagnosis is performed (T_2 , time between emergence and detection). In most studies, this approach is based on back-tracking mutations with a mathematical modeling based on constant rate of mutation occurrence (i.e. age independence)³⁻⁵. Our approach to better define T_1 and T_2 times was rather based on real life registries of MPN and age of pathology detection in patients (ie time when the tumor mass reaches a size allowing diagnosis) just like previously proposed for CML emergence modeling based on Japanese atomic bomb survivor data in Hiroshima⁶ but using larger cohorts of patients. We tested different models of T_1 and T_2 to better define MPN development. Using rigorous statistical arguments, we demonstrate here that the models that best explain the data of both MPN registries we studied, requires that the T_1 active mutation rate relies upon age conversely to all previous models developed, and T_2 is either constant or a lognormal random variable with small variance. Our statistical study allows us to assess the time of emergence and development of MPN. So we demonstrate that the mean time for cancer cell to emerge is 63 years and time from tumor emergence to diagnosis is approximately 8.8 years in accordance with previous hypothesis⁶⁻⁷.

RESULTS

Incidence and frequencies of MPN according to age.

Cancer registry of the Côte d'Or in France gives us the opportunity to study patients diagnosed with different types of MPN from 1990 to 2020 according to the type of driver mutation for each pathology and where life expectancy (and then relative incidence of pathology) can be analyzed. We firstly adjusted the data to take into consideration patients that could have died before being diagnosed and only considered patients with JAK2V617F mutation (Figure 1A-1B). We divided the frequencies of MPN diagnosis at each age by the probability of survival at this age based on the French and European survival data by age and sex of 2021⁸. The corrected data give the

probability to develop JAK2V617F MPN (except Myelofibrosis) for patients who have not died of anything else before. The corrected data indicate that the frequencies of JAK2V617F MPN development increases dramatically in older ages. Once the corrected data set were obtained, we considered different models and analyzed their compatibility with the JAK2V617F MPN set of data. Modeling mutation occurrence and mutation expansion. We postulated two periods T_1 and T_2 : the first one being the time from embryonic development for the mutation to occur, not disappear, and enter in proliferation (that we will name “mutation occurrence”) and a second time corresponding to the expansion time, once the first cancer cell begins to proliferate until the time of MPN diagnosis. To define the first period of time T_1 , we first assumed that the rate of mutation or activation of an existing mutation is constant and equal to τ . This approach was the one that has been used in the majority of genetic analysis backtracking reported to date. We considered that each activated mutant cell has a probability p to proliferate and then be detected. The number $(1-p)$ corresponds to the frequency of non proliferating mutant cells (just like clonal hematopoiesis does for a long period of time) or of mutant cells whose lineages disappear before reaching detection time of MPN. Under these assumptions, T_1 is an exponential random variable with parameter $\delta = \tau p$ (see supplementary information). The time T_2 was first assumed to be constant and the total time $T_1 + T_2$, which is the age of detection, is then distributed as a shifted exponential law. The shift T_2 is a value between 0 and the minimum age of diagnosis in our cohort. We estimated the parameters δ and T_2 of the model. Figure 2A-2B illustrates the data of clinical incidence of MPN in real life compared to the estimation, showing a large disparity between the model and the data. Then, we performed a statistical test to study the hypothesis that the data follow the distribution of our model and found that it was rejected at a 99% significance level, indicating that a constant occurrence rate together with constant expansion time does not fit with the clinical data.

Relaxed assumptions on mutation emergence or expansion time

In an attempt to properly explain the clinical incidence of MPN in the Côte d’Or cohort, we considered relaxed models that allow additional types of variability: individual variability on cancer cell emergence or influence of environment on cancer development. The first model took into account individual variability allowing the time of mutation occurrence to vary from one patient to another or the mutation to develop at different times from one patient to another (quiescence/ cycling). This takes into consideration that the biological hypothesis of stress (or environment) influences cancer cell emergence. This model considered T_1 as an exponential random variable, with its rate being different from one patient to another, and T_2 as a constant. This hypothesis was mathematically rejected based on our data (Figure 2C). (see supplementary information for details). A second model considered that external factors may not influence the emergence but rather the expansion time and the time of detection. Then, the occurrence of JAK2V617F mutation (the T_1 rate $p\tau$ of mutation occurrence) is fixed and constant when T_2 , the expansion time of cancer development is the target of invasion process modifications (ie variation time between two divisions), environment modifications or randomness in the diagnostic process (some patients are diagnosed after vascular events (late detection) when others are diagnosed after a systematic blood cell analysis performed for another pathology (early detection)) or some subjects die (of other unrelated pathologies) before T_2 was finalized. This model combines an exponential random time for mutation occurrence and a lognormal random time for expansion. This hypothesis was also rejected at 99% confidence level (Figure 2D-2E)(see supplementary for details). These model rejections suggest that the active mutation occurrence δ is not constant even when including individual or environmental variations, but is dramatically increasing with age. Thus, alternative models based on increasing probability of JAK2V617F cancer cell emergence with age were mandatory.

Age-dependency of JAK2V617F mutation emergence.

We added an age dependency to the active mutation rate with fixed T_2 . This could be related to at least three biological explanations based on age-dependent modifications of the environment: a time dependency of i-JAK2V617F mutation appearance (from embryo to adulthood), ii- JAK2V617F activation (ie stem cell quiescence exit) or iii- the success probability of the

expansion after activation. As illustrated in Figure 3A-3B, this model could explain our data. We confirmed this by performing a goodness-of-fit test to study the hypothesis of the data following our age-dependent model. With a high power, this test does “not reject” this hypothesis.

Age-dependency of JAK2V617F mutation emergence with different models of tumor growth.

Once T_1 has been defined as age-dependent, different models of tumor growth (T_2) can be postulated. The simplest one was a constant expansion time and we saw that this model could explain our data. A more complex scenario could be postulated with a variable expansion time from one patient to another, due for instance to environmental effects on tumor growth. As previously, we assumed that T_2 follows a unimodal law through a lognormal distribution as suggested before by our group in a Markovian context⁹ and tested if high variation of expansion time could better explain the data (Figure 3C-3D). When the Bayesian information criterion (BIC) was used, the gain of adding variability to T_2 as a lognormal random variable was not significant, suggesting that the simplest first model should be chosen (see supplementary). This suggests that environment modifications (or other sources of variability) do not have a huge impact on the growth phase of the tumor. Based on our registry data, it was possible to calculate the values of the different parameters of the distributions of T_1 and T_2 . The expected occurrence time T_1 is 63 +/- 13 years. The pathology development when this JAK2V617F stem cell is present, fixed and ready to proliferate is 8.8 years (T_2).

Validation of the model in an external cohort.

The French group of MPN developed recently a national database on ET and PV. (BCB-FIMBANK: French National Cancer Institute (INCa) BCB 2013 and 2022, CHU Angers). We used this database, because of the high number of reported MPN, to differentially analyze ET and PV patients. However, because this database is not exhaustive, the incidence of these pathologies in the entire population cannot be calculated. Information concerning the pathologies (ET versus PV versus other MPN), sex, age at diagnosis, driver molecular event, (table 1) were considered as representative of their incidence in the general population because of the data size (n=1111 JAK2V617F MPN patients) (Figure 1C-1D). We then validated our model on this second set of data based on life expectancy in France. (see figure 4A-4B).

Differential analysis of Essential thrombocytemia and polycythemia Vera. To take into account the difference between ET and PV, we differentially analyzed ET and PV cohorts. We hypothesized that ET and PV have a different kinetic because of the double hit in PV (i.e. homologous recombination or development of secondary mutations that induces the polycythemia instead of the thrombocytosis only) compared to single hit in ET. We then compared ET and PV corrected data. Using a comparison chi-2 test, we confirmed that the diagnostic age distributions are different for ET and PV (at a 99% confidence level), PV taking approximately 1.5 years more than ET to develop. (see supplementary).

DISCUSSION

Our present work provides a mathematical modeling based on real life incidence and age at diagnosis of JAK2V617F MPN which highlights the role of age dependence of mutation occurrence in MPN. Based on the regional exhaustive registry of Côte d’Or (France), and lastly validated in a MPN national registry (BCB-FIMBANK registry), we mathematically defined the occurrence and expansion times of JAK2V617F MPN. Most of the previous works performed to decipher the time of JAK2V617F “first” cell appearance, are based on genetic hierarchy and back-tracking performed on ancient blood samples or bone marrow samples. These genetic approaches rely upon premises of a rate (a frequency) of mutation occurrence as yet unknown in MPN. It necessitates old blood or bone marrow samples for genetic analysis (to recapitulate the genetic tree evolution of the initial cancer cell) which is obviously very rare and probably biased¹⁰. Genetic analysis inference performed in such approaches are based on mutation appearance but not necessary proliferative / oncogenic. Indeed, it is now well documented that

such JAK2V617F mutations could stay for long time without development of pathologies. This is well documented in CHIP. Moreover, these genetic back-tracking approaches were built on stable mutation frequencies that overestimate the time of emergence if mutation rate during life is not constant. On the contrary, our approach was based on registry analysis, differing from classical genetic back-tracking of mutation emergence. We systematically developed models based on species evolution modeling using progressively complexified mathematical models. We assumed that two periods of time were necessary to develop and diagnose MPN: a first time period (T_1) corresponding to the mutation acquisition (genetic event from the conception of the embryo) but also its activation (ie: ensuring to develop). This first period of time biologically can correspond to a cell cycle entry of a long-lasting quiescent cell for example, but also includes the possibility of a MPN cancer cell to disappear due to the cancer cell extinction probability. The second time period (T_2) corresponds to the growth and development of such cancer stem cell until diagnosis. This type of modeling has been applied to invasion-fixation of mutants in eco-evolutionary models^{11–13} and to the infectious diseases propagation^{14–15} but less frequently to cancer emergence and development. Most reported modeling assumes that mutation and invasion rate are aging independent (i.e. a fixed rate of mutation and activation and a fixed probability of emergence of the pathology for a given patient), which would imply that T_1 follows an exponential law. However, these models hypothesized a memoryless system whereas (at least) Polycythemia Vera emergence necessitating two successive molecular modifications (JAK2V617F mutation at an heterozygous state followed by allele recombination, a molecularly independent phenomenon from the mutation emergence) suggests a different mechanism. We then speculated that myeloproliferative neoplasm emergence could need an age-dependent modeling for T_1 , meaning a mathematical model that is not as simple as an exponential law as reported in previous models. We also demonstrated this for ET emergence even if there is only one oncogenic event. Age dependence does not necessarily mean that the JAK2V617F mutation acquisition is higher in aged stem cells than in young ones; It also could be interpreted as a mutation appearance during childhood or even before birth, but an activation due to external stimulus long time after. The second time (expansion time) is easier to characterize. Surprisingly, a model considering the expansion time T_2 as a constant properly fits the data. This suggests that external changes (stress, food, toxic exposure...) could not significantly modify the behavior of MPN development and that the proliferation time from one “active” cancer cell to the total mass of cancer at diagnosis is relatively fixed. This could mean that the main determining factor is the proliferative speed related to the mutation acquisition. We then can speculate about the possibility (and risks and benefits) to treat subjects with JAK2V617F clonal hematopoiesis to delay the emergence of the MPN or prevent the classical thrombotic complications related to these pathologies. Based on the Variant Allele Frequency of JAK2V617F in the “FIMBANK” cohort, we can speculate that the mean JAK2V617F VAF in MPN is around 30% (19.9% in ET and 46.1% in PV respectively) and an increased ratio of 1.4% per year (as reported previously in untreated¹⁶ or Hydroxyurea only treated patients¹⁷, this should mean a 10-year period of time from undetectable VAF to the 30% allele ratio observed at diagnosis in our MPN cohort. This is very close (and a little bit higher) to the 8.8 years of tumor expansion time to MPN diagnosis that we calculated in our model. In conclusion, we demonstrated using mathematical modelling that the occurrence (emergence + fixation) of JAK2V617F mutation is linked to aging mechanisms and that the expansion time of MPN is almost fixed and approximately 8.8 years. Our modeling fits well with the JAK2V617F CHIP that has been described to take approximately a decade to transform to MPN^{18–20}. Altogether, these data highlight the interest to test all 50–60 years-old inhabitants for JAK2V617F CHIP and the place of preventive therapies for such subjects.

REFERENCES

1. D. Luque Paz, R. Kralovics, R.C. Skoda, Genetic basis and molecular profiling in myeloproliferative neoplasms. *Blood* **141**, 1909-1921 (2023).
2. P.J. Hurley Red cell and plasma volumes in normal adults. *J Nucl Med.* **16**, 46-52 (1975).
3. N. Williams *et al.*, Life histories of myeloproliferative neoplasms inferred from phylogenies. *Nature* **602**, 162-168 (2022).
4. H. Lee-Six *et al.*, Population dynamics of normal human blood inferred from somatic mutations. *Nature* **561**, 473-478 (2018).
5. F.G. Osorio *et al.*, Somatic Mutations Reveal Lineage Relationships and Age-Related Mutagenesis in Human Hematopoiesis. *Cell Rep.* **25**, 2308-2316 (2018)
6. T. Radivoyevitch, L. Hlatky, J. Landaw, R.K. Sachs. Quantitative modeling of chronic myeloid leukemia: insights from radiobiology. *Blood* **119**, 4363-4671 (2012).
7. T. McKerrell *et al.* JAK2 V617F hematopoietic clones are present several years prior to MPN diagnosis and follow different expansion kinetics. *Blood Adv.* **1**, 968-971 (2017).
8. INED, Data from “Taux de mortalité par sexe et age INED”, Available at <https://www.ined.fr/fr/tout-savoir-population/chiffres/france/mortalite-cause-deces/taux-mortalite-sexe-age>, 2021
9. V. Bansaye, X. Erny, S. Méléard. Sharp approximation and hitting times for stochastic invasion processes, arXiv [Preprint] (2023). <https://arxiv.org/abs/2212.14320> (accessed 14 March 2024)
10. P. Hirsch *et al.*, Clonal history of a cord blood donor cell leukemia with prenatal somatic JAK2V617F mutation. *Leukemia* **30**, 1756-1759 (2016).
11. N. Champagnat, R. Ferrière, S. Méléard, Unifying evolutionary dynamics: From individual stochastic processes to macroscopic models. *Theor. Popul. Biol.* **69**, 297-321 (2006).
12. N. Champagnat, A microscopic interpretation for adaptative dynamics trait substitution sequence models. *Stochastic Process. Appl.* **116**, 1127–1160 (2006).
13. S. Billiard, C. Smadi, The interplay of two mutations in a population of varying size: a stochastic eco-evolutionary model for clonal interference. *Stochastic Process. Appl.* **127**, 701-748 (2017).
14. A. D. Barbour, G. Reinert. Approximating the epidemic curve. *Electron. J. Probab.* **18**, 1-30 (2013)
15. A. D. Barbour, K. Hamza, H. Kaspi and F. C. Klebaner. Escape from the boundary in Markov population processes. *Adv. Appl. Probab.* **47**, 1190-1211 (2015).
16. B.L. Stein *et al.*, Sex differences in the JAK2 V617F allele burden in chronic myeloproliferative disorders. *Haematologica* **95**, 1090-1097 (2010).
17. J.J. Kiladjan *et al.*, Long-term outcomes of polycythemia vera patients treated with ropeginterferon Alfa-2b. *Leukemia* **36**, 1408-1411 (2022).

18. C. Nielsen, H.S. Birgens, B.G. Nordestgaard, L. Kjaer, S.E. Bojesen. The JAK2 V617F somatic mutation, mortality and cancer risk in the general population. *Haematologica* **96**, 450-453 (2011).
19. C. Nielsen, H.S. Birgens, B.G. Nordestgaard, S.E. Bojesen. Diagnostic value of JAK2 V617F somatic mutation for myeloproliferative cancer in 49 488 individuals from the general population. *Br J Haematol.* **160**, 70-79 (2013).
20. I.A. van Zeventer *et al.*, Evolutionary landscape of clonal hematopoiesis in 3,359 individuals from the general population. *Cancer Cell* **41**, 1017-1031 (2023).

Figures

Figure 1: Myeloproliferative cohort descriptions

A: Incidence by age of JAK2V617F Classical MPN (ET and PV, excluding myelofibrosis) in the Cote d'Or Regional Registry Database. **B:** Incidence by age of JAK2V617F classical MPN (ET and PV, excluding myelofibrosis) in the Cote d'Or Regional Registry Database after adjustment excluding other causes of death before the MPN diagnosis. **C:** Incidence by age of JAK2V617F Classical MPN (ET and PV, excluding myelofibrosis) in the National BCB-FIMBANK Cohort. **D:** Incidence by age of JAK2V617F classical MPN (ET and PV, excluding myelofibrosis) in the National BCB-FIMBANK Cohort after adjustment excluding other causes of death before the MPN diagnosis. **E:** Frequencies of JAK2V617F ET (red line) and JAK2V617F PV (blue line) by age at diagnosis in the National BCB-FIMBANK Cohort.

Figure 2: Comparison between data from the Cote d'Or Regional Registry Database and models with constant active mutation rate

A: Frequency of cases for the data (in black) and probability density function of the estimation (in red) for the classical model (T_1 according to constant mutation and mutation activation rates and T_2 being constant) **B:** Accumulated frequencies of cases for the data from the (black) and cumulative distribution of the estimation (in red) for the classical model. **C:** Accumulated frequencies of cases for the data (in black) and 90% confidence interval of the estimation (in red) for the classical model with individual variability (T_1 considered as an exponential random variable, with its rate being different from one patient to another, and T_2 as a constant). **D:** Frequency of cases for the data (in black) and probability density function of the estimation (in red) for the classical model with lognormal MPN growing time (T_1 according to constant mutation and mutation activation rates and T_2 taken as a lognormal random variable) **E:** Accumulated frequencies of cases for the data (in black) and cumulative density of the estimation (in red) for the classical model with lognormal MPN growing time.

Figure 3: Comparison between data from the Cote d'Or Regional Registry Database and models with aging

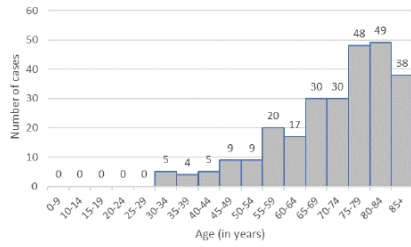
A: Frequency of cases for the data (in black) and probability density function of the estimation (in red) for the model with aging (T_1 according to age-dependent mutation and mutation activation rates and T_2 being constant) **B:** Accumulated frequencies of cases for the data (black) and cumulative distribution of the estimation (in red) for the model with aging **C:** Frequency of cases for the data (in black) and probability density function of the estimation (in red) for the model with aging and lognormal MPN growing time (T_1 according to age-dependent mutation and mutation activation rates and T_2 taken as a lognormal random variable) **D:** Accumulated frequencies of cases for the data (black) and cumulative distribution of the estimation (in red) for the model with aging and lognormal MPN growing time.

Figure 4: Comparison between data from the National BCB-FIMBANK Cohort and the model with aging

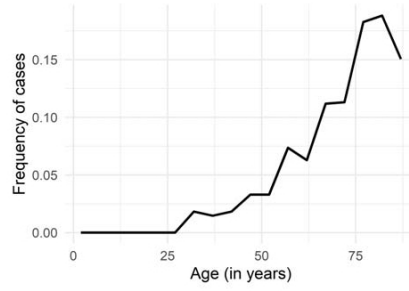
A: Frequency of cases for the data (in black) and probability density function of the estimation (in red) for the model with aging (T_1 according to age-dependent mutation and mutation activation rates and T_2 being constant) **B:** Accumulated frequencies of cases for the data (black) and cumulative distribution of the estimation (in red) for the model with aging.

Table 1: Information concerning the pathologies ET versus PV by sex

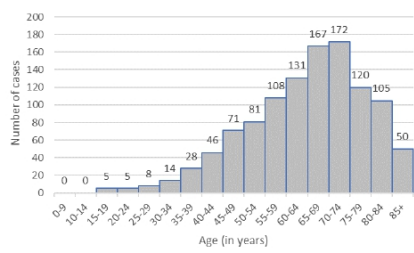
1.A



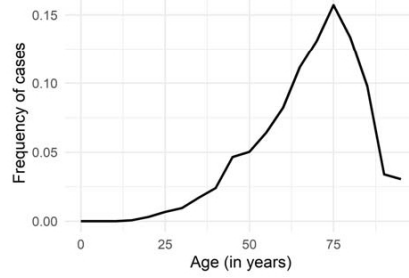
1.B



1.C



1.D



1.E

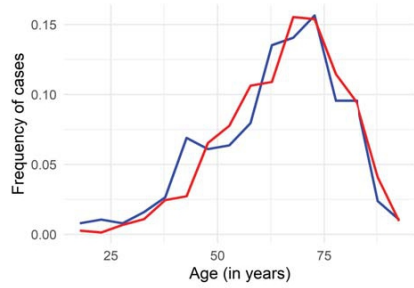
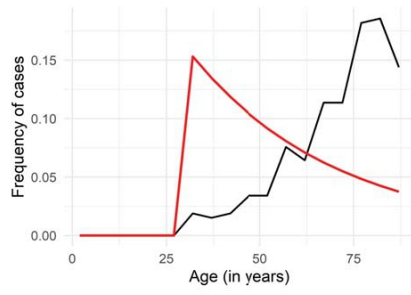
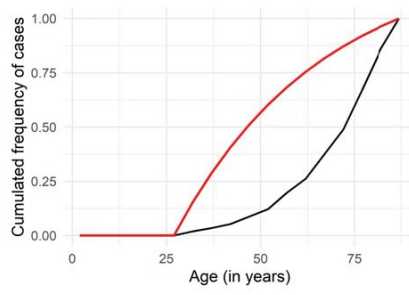


Figure 1

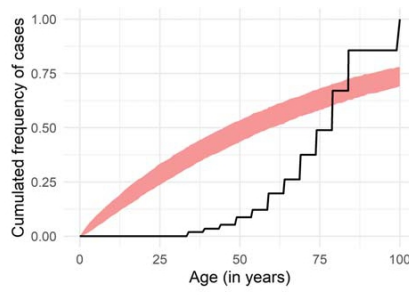
2.A



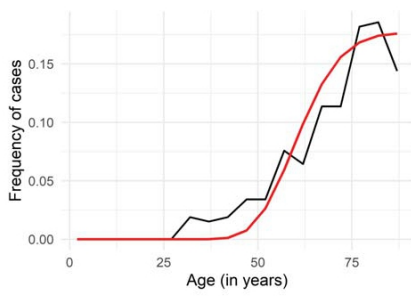
2.B



2.C



2.D



2.E

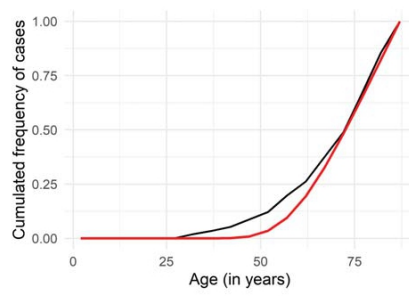
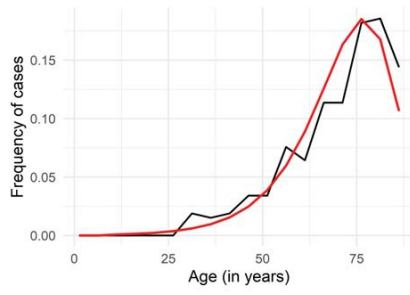
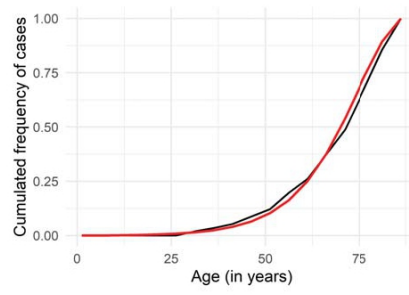


Figure 2

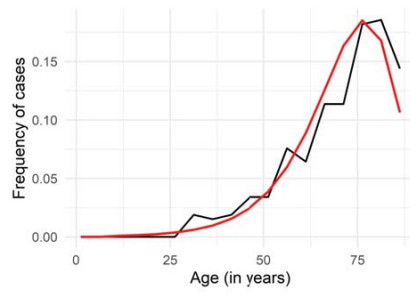
3.A



3.B



3.C



3.D

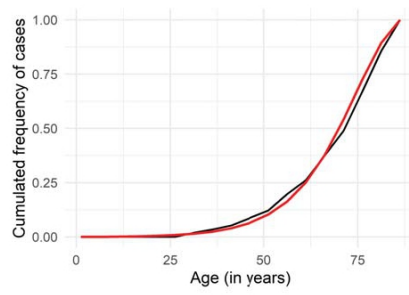
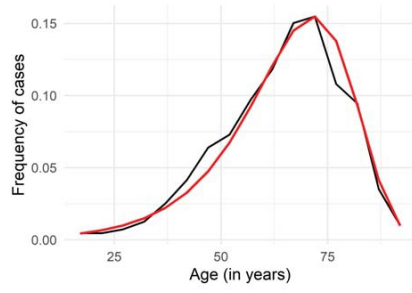


Figure 3

4.A



4.B

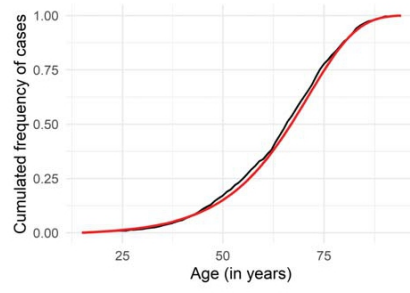


Figure 4

		Number of cases	Mean age at diagnosis	Standard deviation of age	VAF JAK2V617F at diagnosis	Standard deviation of VAF
PV	Female	314	66.7	13.7	45.3	22.9
	Male	421	64.0	13.3	46.7	30.3
ET	Female	229	63.0	15.9	19.2	5.7
	Male	147	63.2	13.8	20.9	15.8

Table 1

Supplementary information for: Classical Myelo-Proliferative Neoplasms emergence and development based on real life incidence and mathematical modeling

Ana Fernández Baranda, Vincent Bansaye, Evelyne Lauret, Morgane Mounier, Valérie Ugo, Sylvie Méléard, and Stéphane Giraudier

Introduction

This work centers around studying the evolution through time of the size of a cancer cell population in an individual. In particular, the goal is to estimate the distribution of the age of detection for myeloproliferative disorders (MPD), that is, blood cancers. The MPD studied are Essential Thrombocytemia and Vaquez disease, both for cases presenting the JAK2V617 mutation. This mutation occurs in stem cells level and is carried in its descendance. A medical observation used throughout this study is that cancer is detected when the number of JAK2V617F cells is over $M = 10^{12}$. The focus was on the age of detection denoted by T_M . Time to detection, T_M was considered to be composed of two independent elements:

$$T_M = T_1 + T_2,$$

where

- T_1 : active mutation time, that is, the time to appear and enter proliferation for the first JAK2V617F stem cell whose lineage will reach detection size;
- T_2 : growing time from the first proliferative JAK2V617F stem cell to the diagnosis of MPN (MPN growing time).

These two times were taken as independent since the time taken for a cell to become active, should not be related to the time for its population to grow to a certain size.

In order to consider that the JAK2V617F could have happened at an embryonic level, as suggested in (Mosca et al., 2021). T_M was considered to start 9 months before the birth of an individual.

The models studied in this work for the age of detection of MPN can be divided into two categories: ones that consider that the active mutation rate is constant, and ones that consider it to be dependent on the age of the individual. The first category of models were analysed under different assumptions and we found that they do not seem to be appropriate to explain significantly (from the statistical point of view) the data available. The second type of models, under the assumption that the active mutation rate grows with age, suggested a much better fit to the data, in particular when considering time for the disease to reach detection size as having some variability.

Data

The data used in this work corresponds to the age of detection of different MPD in the presence of JAK2V617F mutation in the Côte d'Or region in France.

The data set contains summarized data in age ranges for 264 individuals presenting JAK2V617F mutation and attained with one of three MPD: Primary myelofibrosis (PMF), Primary Polycythemia (Vaquez disease (PV)) and Essential thrombocytosis (ET). Table 1 shows this information. The total ages of detection have a mean of 71.9 years and a standard deviation of 13.8 years.

To further validate the models another set from FIMBANK was used, containing the ages of detection for ET and PV of 1111 individuals as seen in Table 2. This gives a mean for the total number of cases of 64.4 years and a standard deviation of 14.1 years.

The two sets of data given here were adjusted to take into account the distribution of the population into each age group and consider the proportion of individuals diagnosed within each group. This considers that some individuals could have died before being diagnosed and thus not present in the data sets. Each frequency was then divided by the probability of survival up to that age group.

For an individual to be diagnosed at age t , it has to also be alive, that is to die after detection. Let T_D be the time of death, then the frequencies obtained by the data of the probability of being detected at age t is

$$\mathbb{P}(T_M = t, T_D \geq t),$$

if we suppose independence between the two variables, this is equal to

$$\mathbb{P}(T_M = t)\mathbb{P}(T_D \geq t)$$

Using the death rates for each age group, one can obtain $\mathbb{P}(T_D \geq t)$ and then calculate

$$\mathbb{P}(T_M = t) = \frac{\mathbb{P}(T_M = t, T_D \geq t)}{\mathbb{P}(T_D \geq t)}.$$

Models with constant active mutation rate

Exponential distribution of T_1

The first hypothesis considered, which is commonly found in literature (Mosca et al., 2021) (Van Egeren et al., 2021) (Mitchell et al., 2022), was that that mutations from stem cells occur at a constant rate τ and each mutant cell has a probability p of eventually having its population reach detection size. $1 - p$ is then the probability of a mutation either not being towards a cancer cell or being towards a cancer cell and its lineage dying out before reaching size M .

To find the law of T_1 , let L be a random variable of law $Geom(p)$ that corresponds to the number of mutation attempts before the first active cancer cell appears. Let X_1, X_2, \dots be independent identically distributed random variables of law $Exp(\tau)$ that define the time taken between every mutation attempt. Then, the law of T_1 is defined as follows

$$T_1 = \sum_{i=1}^L X_i,$$

that is, T_1 corresponds to the sum of the times between each mutation attempt until the appearance of a JAK2V617F cell who's lineage won't die out.

The law of this variable can be found using the generating function

$$\begin{aligned} \mathbb{E}[e^{-\lambda T_1}] &= \mathbb{E}[\mathbb{E}[e^{-\lambda T_1} | L]], \\ &= \mathbb{E}\left[\left(\frac{\tau}{\tau - \lambda}\right)^L\right], \\ &= \sum_{k \geq 1} \left(\frac{\tau}{\tau - \lambda}\right)^k p(1 - p)^{k-1}, \\ &= \left(\frac{\tau}{\tau - \lambda}\right) p \sum_{k \geq 1} \left(\frac{\tau(1 - p)}{\tau - \lambda}\right)^{k-1} \\ &= \left(\frac{\tau}{\tau - \lambda}\right) p \frac{\tau - \lambda}{\tau - \lambda - \tau(1 - p)} \\ &= \left(\frac{\tau p}{\tau p - \lambda}\right). \end{aligned}$$

Hence, $T_1 \sim \text{Exp}(\delta)$ with $\delta = \tau p$. And its law is given by

$$f_1(t) = \delta e^{-\delta t}. \quad (1)$$

Under the hypothesis of a constant active mutation rate three models were studied: MPN growing time was studied as a constant and as a random variable and individual variability was considered on the active mutation time (T_1).

Classical model: Constant active mutation rate for T_1 and constant T_2

Starting with a simple model that will later be complexified, one can consider $T_2 = \alpha$, $\alpha \in [0, \gamma]$ with γ being the smallest age of detection. This would imply that once the active mutation appears, the time for the population to reach detection size is always the same, no matter what. Then, $T_M = T_1 + T_2 = T_1 + \alpha$, and the law of T_M is a shifted exponential, that is

$$f_M(t) = \delta e^{-\delta(t-\alpha)}. \quad (2)$$

The least squares estimation for the parameters of this model using the first data set found in Table 1 was obtained using the function `fitdist()` on R and gives

$$\delta = 0.0256, \quad \alpha = 32.$$

Then, the mean and standard deviation of the distribution of T_M are

$$\mu = \frac{1}{\delta} + \alpha = 71.1, \quad \sigma = \frac{1}{\delta} = 39.03.$$

When comparing these values to the ones in the first data set in Table 1, the mean is close (71.9), but the standard deviation (13.8) is around three times more. Then, the model gives a distribution that is much more spread than the one in the data. The model seems to follow the opposite trend as the data: it gives a strong probability to small ages, while the data is more focused in older ages (see Figure 2A-2B of the main paper).

This leads us to believe that it is not an appropriate model for this type of data. To confirm this idea, a Chi-square test can help study if the model fits the data. In particular, the hypotheses considered are

$$\begin{aligned} \mathcal{H}_0 &= \text{the data follows the distribution of the classical model (2),} \\ \mathcal{H}_1 &= \text{the data do not follow said distribution.} \end{aligned}$$

To apply a Chi-square statistic, consider the $k = 12$ bins already existing in the data, corresponding 5 year increments from age 30 to 85 and 85+.

The test results in rejecting the null hypothesis at a 95% confidence level with a p-value smaller than 10^{-17} .

This confirms that it seems very unlikely that such a model could explain the data. There could be different factors as to why this model did not fit the data. Continuing under the assumption of a constant parameter δ , we studied two other different scenarios: consider T_2 as a random variable and the addition of individual variability.

Classical model with lognormal MPN growing time: Constant active mutation rate for T_1 and random T_2

When taking T_2 as a fixed number, it would mean that the time for the population to reach detection size is always the same. In order to relax this hypothesis, T_2 is now taken as a random variable that follows a lognormal distribution with parameters (μ, σ^2) . This distribution was used since the values of T_2 need to be positive and considered the assumption that they center around

a value. In this scenario, time to development is centered around a value, yet presents a certain variability. Under this assumptions, since T_1 and T_2 are independent, the law of T_M is given by

$$f_M(t) = \int_0^t f_1(s)f_2(t-s)ds,$$

with

$$f_2(t) = \frac{1}{t\sigma\sqrt{2\pi}} \exp\left(-\frac{(\log(t) - \mu)^2}{2\sigma^2}\right), \quad (3)$$

and f_1 as in equation (1). This implies that

$$f_M(t) = \int_0^t \delta e^{-\delta s} \frac{1}{(t-s)\sigma\sqrt{2\pi}} \exp\left(-\frac{(\log(t-s) - \mu)^2}{2\sigma^2}\right) ds. \quad (4)$$

A least square estimation can be used to estimate the parameters of the model for the data in Table 1 with the function `fitdist()` on R, giving as results

$$\delta = 0.0011, \quad \mu = 4.11, \quad \sigma = 0.15.$$

The model seems closer to the data than the classical model without random MPN growing time (2), but still far from it (see Figure 2D-2E of the main paper).

To confirm if the model fits the data, a Chi-square test is used with a significance level of 5%.

The hypotheses considered are

\mathcal{H}_0 = the data follows the distribution of the classical model with lognormal MPN growing time (4),

\mathcal{H}_1 = the data does not follow said distribution.

The test results in rejecting the null hypothesis with a p-value smaller than 10^{-17} .

Hence, considering T_2 as a random variable does not allow us to explain the data.

Classical model with individual variability: Constant active mutation rate for T_1 individual variability and constant T_2

A possible explanation of why the classical model ((2)) failed to describe the data is that there are different intrinsic and environmental factors in each individual that make it more or less likely for them to get an active mutation.

In order to consider individual variability in the classical model, the population approach can be used. Allowing each individual to have a different active mutation rate δ_i , $i = 1, 2, \dots, N$, one can then assume that each age of detection Y_i is drawn from an exponential distribution with parameter δ_i . The δ_i 's are considered as a sample of a *lognormal*(m, s^2). The lognormal distribution was used since it gives positive values, and is unimodal, meaning that it centers around a value, but presents variability. The population parameters corresponding to the mean and variance of the Y_i 's are

$$\delta_{pop} = \exp\left(m + \frac{s^2}{2}\right), \quad \omega_{pop} = \exp(2m + s^2) (\exp(s^2) - 1).$$

This model considers that the law of T_M is an exponential with a shift, same as before, but the parameter δ of the law is different from individual to individual.

The estimation of the parameters δ_{pop} and ω_{pop} according to the data in Table 1 was done using Monolix, (Lavielle, 2014), a software that is well adapted for this approach. It allows to easily make an estimation of the parameters when considering the survival analysis approach. It is based on the SAEM algorithm and gives robust and global convergence. It gives the results

$$\delta_{pop} = 0.022, \quad \omega_{pop} = 0.16.$$

The estimation of the model does not follow at all the data (see Figure 2C of the main paper). Hence, it is very unlikely that our data follows the classical model with individual variability. The classical model considering a constant active mutation rate for T_1 does not seem to properly explain the data. Considering this, one can think that it is unlikely that such an assumption is true with the data considered. Hence, a dependency on the age of the individual seems needed to be able to model the age of detection.

Models with time dependency of the active mutation rate

Model with aging: Age dependency of active mutation rate for T_1 and constant T_2

This section centers around the study of a time dependency of the parameter δ , meaning that as a person gets older, it would be more likely for them to develop a mutation or for a mutation to be active. The parameter δ is taken as a function of time, in particular

$$\delta(t) = A \exp(kt),$$

such that $\delta(t) > 0$ for $t > 0$. This shape for the parameter δ was considered since it's commonly seen in literature (Lavielle, 2014) and allows to cover different types of functions, for example, for k very small, $\delta(t)$ resembles an affine function.

With this rate, the law of T_1 is given by

$$f_1(t) = A \exp\left(\frac{A}{k}\right) \exp(kt) \exp\left(-\frac{A}{k} \exp(kt)\right). \quad (5)$$

The study starts again with a simple case by taking $T_2 = \alpha$, $\alpha \in \mathbb{R}^+$. This would imply that the time for the mutant cells population, once the first active JAK2V617F cell appears in the system, to reach detection size, is fixed and the same for all individuals. Under these assumptions, the law of T_M is the shifted law of T_1 as in equation (5), that is,

$$f_M(t) = A \exp\left(\frac{A}{k}\right) \exp(k(t - \alpha)) \exp\left(-\frac{A}{k} \exp(k(t - \alpha))\right). \quad (6)$$

The estimation of the parameters A , k and α is done using an EM algorithm as explained in Mathematical tools and gives the following values for the data in Table 1

$$A = 0.000124, \quad k = 0.096577, \quad \alpha = 8.76.$$

With these values, the mean of T_1 is 63.1 years and it's standard deviation 13 years.

The distribution of T_M seems much closer to the data than what we had found in the classical models (see Figure 3A-3B of the main paper). In particular, it follows the trend of the data correctly.

To test if the distribution fits the data, consider the hypothesis

$$\mathcal{H}_0 = \text{the data follows the distribution of the model with aging (6),}$$

$$\mathcal{H}_1 = \text{the data does not follow said distribution,}$$

and apply a Chi-square statistic with a 5% significance level. This test fails to reject the null hypothesis. The power of the test is of $1 - \beta = 0.952$, implying that the type II error probability is of $\beta = 0.048$, more information on this value can be seen in Mathematical tools.

While these results could indicate that the data is properly explained by the data, it is of interested to study if the addition of a random T_2 gives a better fit.

Model with aging and lognormal MPN growing time: Age dependency of active mutation rate for T_1 and random T_2

In the previous model with aging (6), time to detection once the mutation appears was considered as fixed. This would mean that for each individual, the JAK2V617F cells develop in the same way, reaching detection size in a specific time. It would make sense to loosen this assumption and consider some variability in this time as in in the classical model. In the same way, the time T_2 can then be taken as a random variable such that $T_2 \sim \text{lognormal}(\mu, \sigma^2)$ with the distribution of (3).

Then, the law of T_M is given by

$$f_M(t) = \int_0^t f_1(s)f_2(t-s)ds,$$

since T_1 and T_2 are independent. That is

$$f_M(t) = \int_0^t A \exp\left(\frac{A}{k}\right) \exp(ks) \exp\left(-\frac{A}{k} \exp(ks)\right) \times \frac{1}{(t-s)\sigma\sqrt{2\pi}} \exp\left(-\frac{(\log(t-s) - \mu)^2}{2\sigma^2}\right) ds \quad (7)$$

The estimation of the parameters A , k , μ , σ^2 using an EM algorithm corresponding to the data in Table 1, gives the following approximations

$$A = 0.000122, \quad k = 0.095814, \quad \mu = 2.083590, \quad \sigma = 0.099585.$$

This corresponds to a mean for T_2 of 8.07 years and a standard deviation of 0.81 years.

The distribution of T_M with these values compared to the data can be found in Figure 3C-3D of the main paper. It seems to also fit the data well.

To test if the distribution fits the data, consider the hypothesis

\mathcal{H}_0 = the data follows the law of the model with aging and lognormal MPN random time(7),

\mathcal{H}_1 = the data does not follow said distribution,

and apply a Chi-square statistic with a significance level of 5%. This test fails to reject the null hypothesis. The power of the test is 0.85, indicating that the distribution of equation (7) seems to properly explain the data. For more details about the power of a test, check Mathematical tools.

Comparing the two models with aging

When considering a dependency on time of the parameters δ , the Chi-square tests failed to reject that both models with aging with or without a random MPN growing time, fitted the data. In order to select the model that can best describe the data, the Bayesian Information Criterion (BIC) can be used. Its formula is given by

$$\text{BIC} = k \log n - 2 \log \hat{L},$$

where k is the number of parameters of the model, n is the size of the data sample and \hat{L} is the maximized value of the likelihood function, that is

$$L(X, \theta) = \prod_{i=1}^N \mathcal{P}(X_i | \theta).$$

A lower BIC is preferred.

It makes sense that adding variability to T_2 should at least perform as well as the model without it, at least in terms of the likelihood. Yet, the addition of a new parameter to a model could result in overfitting, reason why the BIC penalises the number of parameters through the first term. Calculating the BIC of the models results in

$$\text{BIC}_1 = 2079.048, \quad \text{BIC}_2 = 2085.299,$$

with BIC_1 for the model with aging and constant MPN growing time 6 with T_2 as a fixed value and BIC_2 for the model with aging and lognormal MPN growing time 7. The first model has a lower BIC. These results indicate that while incorporating variability on T_2 gives a better fit to the data, the gain is small and not compensated by the cost of adding a new parameter. This would imply that, given our data, the first model with age dependency is the most appropriate to explain the data under these assumptions.

Validating the model with aging and constant MPN growing time

Given the previous results, it seems that the model with age dependency on the active mutation rate δ and constant MPD growing time T_2 can best describe the distribution of detection age for the Cote d'Or data. To validate this, the second data set (FIMBANK) in Table 2 can be used. The estimation of the parameters using an EM algorithm as described in Mathematical tools, gives

$$A = 0.000439, \quad k = 0.083433, \quad \alpha = 8.8.$$

The model seems to properly fit the data (see Figure 4 of the main paper). To test if the distribution fits the data, consider the hypothesis

$$\begin{aligned} \mathcal{H}_0 &= \text{the data follows the law of } T_M, \\ \mathcal{H}_1 &= \text{the data does not follow said distribution,} \end{aligned}$$

and apply a Chi-square statistic with a significance level of 5%. This test fails to reject the null hypothesis with a power of $1 - \beta = 1 - 2 \cdot 10^{-7}$.

Comparing PV vs ET

PV and ET develop in different ways: while ET presents a majority of heterozygous cells, PV presents mostly homozygous ones. This means that for PV to develop, there needs to be a mitotic recombination in order for the heterozygous cell to become homozygous. Hence, it is of interest to study the difference in time to detection between PV patients and ET patients. To do this, the FIMBANK data was used given its larger size.

Comparing the diseases data

There is not a clear difference between the two diseases (see Figure 1E of the main paper). When looking at their means and standard deviations, PV presents a bigger mean (65.1 years) by 2 years than ET (63.1 years). The standard deviation of ET is bigger by 1.6 years (the standard deviation of PV is 13.5 and of ET 15.1), meaning that the ages of detection are spread across a larger range.

Testing if the both diseases have the same distribution, that is, comparing the hypothesis

$$\begin{aligned} \mathcal{H}_0 &= \text{both data sets come from the same distribution,} \\ \mathcal{H}_1 &= \text{both data sets do not come from the same distribution.} \end{aligned}$$

through a Chi-square test results in rejecting the null hypothesis with a p-value of 10^{-11} . This shows that indeed each disease seems to follow a different trend in terms of ages of detection. To further study this, one can compare the results when considering the selected model for MPNs.

Comparing the parameters for each disease in the model with aging

In order to compare these diseases in terms of T_1 and T_2 , consider the model with aging and constant MPN growing time (7) which is the one that fitted the data best. The resulting of the

estimated parameter values and the mean (m_1) and standard deviation (s_1) of T_1 for each disease are

$$\begin{aligned} A^{PV} &= 0.00037, & k^{PV} &= 0.08575, & T_2^{PV} &= 8.8, & m_1^{PV} &= 56.9, & s_1^{PV} &= 14.2 \\ A^{ET} &= 0.00056, & k^{ET} &= 0.07935, & T_2^{ET} &= 8.3, & m_1^{ET} &= 55.5, & s_1^{ET} &= 15.1 \end{aligned}$$

The mean of T_1 for PV is larger than for TE by almost 1.5 year, which could be explained by the time taken for the mitotic recombination to happen.

Mathematical tools

Generalized EM algorithm

The generalized EM algorithm (Rai and Matthews, 1993) was used to estimate the parameters of some models studied.

Let X be the vector that corresponds to the observed data of ages of detection and has distribution $f_X(x; \theta)$ for an age x . Consider that there is some missing data z , corresponding to the values of T_2 with distribution $f_Z(z; \theta)$. Then the complete data is (x, z) , and is distributed according to $f_{X,Z}(x, z; \theta)$. If the complete data was available, the the log-likelihood could be calculated by

$$\log L_{X,Z}(\theta) = \log f_{X,Z}(x, z; \theta).$$

The generalized EM algorithm works by finding the values of the parameters that maximize this function.

The generalized EM algorithm (McLachlan and Krishnan, 2008) is an iterative algorithm that consists of two steps: the E-step and the M-step. Starting from an initial value θ_0 , then, on iteration $k + 1$, the E-step involves computing

$$Q(\theta; \theta_k) = \mathbb{E}_{\theta_k}(\log L_{X,Z}(\theta) | x).$$

Then, on the M-step choose θ_{k+1} such that

$$Q(\theta_{k+1}; \theta_k) \geq Q(\theta_k; \theta_k).$$

For the M-step, consider the approach of (Rai and Matthews, 1993), were they propose to take θ_{k+1} as one Newton-Raphson step from θ_k over the function $Q(\theta_{k+1}; \theta_k)$, that is

$$\theta_{k+1} = \theta_k + a_k \delta_k,$$

where

$$\delta_k = - \left[\frac{\partial^2(Q(\theta; \theta_k))}{\partial \theta \partial \theta^T} \right]^{-1} \Bigg|_{\theta=\theta_k} \left[\frac{\partial(Q(\theta; \theta_k))}{\partial \theta} \right] \Bigg|_{\theta=\theta_k}$$

and $0 < a_k \leq 1$. The choice of a_k needs to be such that it stays in the parameters space and the likelihood is nondecreasing. To do this, take $a_k^0 = 1$ and divide by half its value until the parameters satisfy the desired conditions, obtaining $a_k^j = 2^{-j}$ as a result. Then, apply backtracking line search ; we starting at a_k^j and while $Q(\theta_k + a_k^i \delta_k; \theta_k) > Q(\theta_k; \theta_k) + 10^{-4} a \nabla Q(\theta_k; \theta_k)^T \delta_k$, set $a_k^{i+1} = 0.8 a_k^i$. Then, take a_k as the final value of these steps.

Chi-square test

The Chi-square test was used to compare different hypotheses thorough this work. Consider data that is gathered into k bins and corresponds to N individuals.

Given a model, first consider the hypotheses

$$\begin{aligned}\mathcal{H}_0 &= \text{the data follows the model distribution,} \\ \mathcal{H}_1 &= \text{the data does not follow said distribution.}\end{aligned}$$

Denote the probability function of the model by $F(x)$, the test statistic is built as follows: (Snedecor, 1967)

- Take X_l^i, X_u^i as the lower and upper bounds of bin i ,
- O_i is the frequency in bin i ,
- For each i , compute $E_i = N(F(X_u^i) - F(X_l^i))$,
- The test statistic is

$$\chi^2 = \sum_{i=1}^k \frac{(O_i - E_i)^2}{E_i}.$$

The null hypothesis is rejected if

$$\chi^2 \geq \chi_{1-\alpha, k-m}^2$$

where m is the number of estimated parameters.

Given two datasets, another type of hypotheses that can be tested is

$$\begin{aligned}\mathcal{H}_0 &= \text{both data sets come from the same distribution,} \\ \mathcal{H}_1 &= \text{both data sets do not come from the same distribution.}\end{aligned}$$

If the sets have different sizes, consider the scaling constants

$$K_1 = \sqrt{\frac{\sum_{i=1}^k S_i}{\sum_{i=1}^k R_i}}, \quad K_2 = \sqrt{\frac{\sum_{i=1}^k R_i}{\sum_{i=1}^k S_i}}$$

where R_i and S_i are the number of cases in bin i for the first and second set, respectively. The test statistic is

$$\chi^2 = \sum_{i=1}^k \frac{(K_1 S_i - K_2 R_i)^2}{R_i + S_i}.$$

The null hypothesis is rejected if

$$\chi^2 > \chi_{1-\alpha, k}^2$$

where k is the number of non-empty bins.

There are two errors that can be made with these type of tests. The type I error corresponds to falsely rejecting the null hypothesis, that is, rejecting \mathcal{H}_0 when it is true. The type II error represents not rejecting the null hypothesis when it is false.

The probability of a type I error is called the significance level α . When the test results in rejecting the null hypothesis, one can evaluate the evidence against the null hypotheses through its p-value: the smallest significance level at which \mathcal{H}_0 would be rejected. The p-value is given by

$$\mathbb{P}(\text{reject } \mathcal{H}_0 | \mathcal{H}_0).$$

Smaller p-values indicate strong proof to reject the null hypothesis. Commonly, it is desired for this value to be smaller than 0.05.

On the other hand, when the test fails to reject the null hypothesis, one can study the power of the test, $1 - \beta$ with β the probability of a type II error. The power represents the probability of rejecting the null hypothesis when it is wrong. The bigger the value of the power, the more significant the results of the test will be.

The power on a goodness of fit Chi square test depends on four values: the size of the data n , the significance level considered in the test α , the degrees of freedom of the test, and the effect size index. The effect size can be calculated as

$$\sqrt{\frac{\chi^2}{n}}$$

with χ^2 the value of the statistic. The power can then be found through the function `pwr.chisq.test()` on R.

Table 1: Number of cases for each age group for the different diseases from the Cote d'Or Regional Registry Database.

Age	PMF	PV JAK2+	ET JAK2+	Total JAK2+ cases
0 to 4	0	0	0	0
5 to 9	0	0	0	0
10 to 14	0	0	0	0
15 to 19	0	0	0	0
20 to 24	0	0	0	0
25 to 29	0	0	0	0
30 to 34	0	1	4	5
35 to 39	0	0	4	4
40 to 44	0	1	4	5
45 to 49	0	5	4	9
50 to 54	0	2	7	9
55 to 59	1	8	11	20
60 to 64	1	10	6	17
65 to 69	2	13	15	30
70 to 74	4	12	14	30
75 to 79	5	14	29	48
80 to 85	4	15	30	49
More than 85	4	11	23	38
Total number	21	92	151	264

Table 2: Number of cases for each age group for the different diseases from the National BCB-FIMBANK Cohort.

Age	PV JAK2+	ET JAK2+	Total JAK2+ cases
0 to 4	0	0	0
5 to 9	0	0	0
10 to 14	0	0	0
15 to 19	2	3	5
20 to 24	1	4	5
25 to 29	5	3	8
30 to 34	8	6	14
35 to 39	18	10	28
40 to 44	20	26	46
45 to 49	48	23	71
50 to 54	57	24	81
55 to 59	78	30	108
60 to 64	80	51	131
65 to 69	114	53	167
70 to 74	113	59	172
75 to 79	84	36	120
80 to 84	69	36	105
85 to 90	30	9	39
90 to 94	7	4	11
Total number	734	377	1111

References

- Lavielle, M. (2014). *Mixed Effects Models for the population Approach: Models, Tasks, Methods and Tools*. second edition.
- McLachlan, G. J. and Krishnan, T. (2008). *The EM Algorithm and extensions*. Wiley-interscience.
- Mitchell, E., Spencer Chapman, M., Williams, N., Dawson, Kevin ad Mende, N., Calderbank, E. F., Jung, H., Mitchell, T., Coorens, T., Spencer, D., Machado, H., Lee-Six, H., Davies, M., Hayler, D., Fabre, M., Mahbubani, K., Abascal, F., Cagan, A., Vassiliou, G., Baxter, J., Green, A. R., Nangalia, J., Laurenti, E., and Campbell, P. J. (2022). Clonal dynamics of haematopoiesis across the human lifespan. *Nature*, 606:343–350.
- Mosca, M., Hermange, G., Tisserand, A., Noble, R., Marzac, C., Marty, C., Le Sueur, C., Campario, H., Vertenoil, G., El-Khoury, M., Catelain, C., Rameau, P., Gella, C., Lenglet, J., Casadevall, N., Favier, R., Solary, E., Cassinat, B., Kiladjian, J.-J., Constantinescu, S., Pasquier, F., Hochberg, M., Raslova, H., Villeval, J.-L., Girodon, F., Vainchenker, W., Cournède, P.-H., and Plo, I. (2021). Inferring the dynamic of mutated hematopoietic stem and progenitor cells induced by ifn - α in myeloproliferative neoplasms. *Blood*, 138:2231–2243.
- Rai, S. and Matthews, D. (1993). Improving the em algorithm. *Biometrics*, 46:587–591.
- Snedecor, G. W. (1967). *Statistical methods*. sixth edition.
- Van Egeren, D., Escabi, J., Nguyen, M., Liu, S., Reilly, C. R., Patel, S., Kamaz, B., Kalyva, M., DeAngelo, D. J., Galinsky, I., Wadleigh, M., Winer, E. S., Luskin, M. R., Stone, R. M., Garcia, J. S., Hobbs, G. S., Camargo, F. D., Michor, F., Mullally, A., Cortes-Ciriano, I., and Hormoz, S. (2021). Reconstructing the lineage histories and differentiation trajectories of individual cancer cells in myeloproliferative neoplasms. *Cell Stem Cell*, 28:514–523.